Research Projects:

標題：由人類胃黏膜細胞誘導的多能性幹細胞探討 HoxA 家族基因於胃癌發展中扮演之角色

摘要

將病人身上取得之細胞誘導成多能幹細胞可用於研究發病機轉及新一代藥物治療之發展，而癌症幹細胞之辨識是一個很重要的新方法以抑制早期癌症的發生，從直覺上推論誘導型多能幹細胞轉變為癌症幹細胞需要經過基因上的修飾、突變才會發生，由於理想的癌症幹細胞應具有自我更新及形成腫瘤的分化潛力，但仍未有分子證據證實誘導型多能幹細胞與癌症幹細胞之間的關聯 一連串的基因突變和腸胃癌症幹細胞表觀基因的修飾會導致連續性的傷害，從而使惡性表型的表現加劇（缺乏 polyposis coli─息肉增生；低度甲基化─管狀腺瘤；K-Ras 突變─管狀絨毛線瘤；結腸癌缺失基因(DCC)─絨毛腺瘤；p53 基因突變─腺癌)。在此，我們著眼於 HoxA 家族基因於癌症幹細胞及 kRas 突變、p53 與 APC 剔除之共同影響下在胃癌發展中所扮演的角色。我們也將建立 kRas 突變、p53 剔除之基因轉殖鼠或 kRas 突變、p53 及 APC 剔除基因轉殖鼠以進一步闡述 HoxA 基因於胃癌發展中的作用。因此，我們用胃黏膜細胞 CSN 與胃癌細胞 CS12 為基礎建立誘導型多能幹細胞（J. Gastroenterology and Hepatology 22, 1460-1468, 2007)並確認其幹細胞特性（目標一），目前已有文獻指出 CS12 細胞的 HoxA 家族基因從第七對染色體位移到第十二對染色體，造成諸如 HoxA5、HoxA7、HoxA9、HoxA13 等 HoxA 基因的表現量增加。病人之誘導型多能幹細胞在經由導入突變的基因或改變其表觀基因修飾後對於產生癌症幹細胞是非常有用的（目標二），而誘導型多能幹細胞對胃癌發展的影響也會經由共培養胃癌細胞 CS12 被驗證（目標三），並且使用分子影像系統分析誘導型多能幹細胞與胃癌幹細胞在胃癌發生時的動向（目標四），而癌症幹細胞在發展成癌症過程中之各時期細胞可被用於藥物的篩選（目標五)。

一、 實驗目的

從 2006 年迄今，已經有許多文獻由小鼠及人類細胞中成功產生誘導多能性幹細胞(誘導型多能幹細胞。現今，我們可以經由適當的臨床前實驗利用誘導型多能幹細胞發展再生醫藥，而由患者細胞誘導成的誘導型多能幹細胞對於病因或發展新一代療法也有貢獻。近來發現，腫瘤中的癌症幹細胞（cancer stem cells, CSCs)擁有足夠自我更新及多潛能的特性，但其失控的增生能力及分化機制失調。以腸癌為例，一連串的突變及表觀基因型改變造成序列損傷而使惡性表型產生，諸如大腸直腸瘜肉-polyposis coli (APC)缺失；管狀腺瘤-甲基化不足；管狀絨毛腺瘤-kRas 突變；絨毛腺瘤-大腸缺損基因（DCC)；腺癌-p53 突變等等。

在此，我們將研究著眼於癌症幹細胞發展成胃癌之 HoxA 基因及誘導型多能幹細胞所扮演的角色，並使用紅外光螢光蛋白與膽綠影像系統追蹤誘導型多能幹細胞或胃癌幹細胞在胃癌發展中之位置，而這些由患者細胞建立的誘導型多能幹細胞對於疾病的發生、胃癌進程各時期之藥物篩選將會非常有幫助。

目的一、胃癌細胞 CS12 及胃黏膜細胞 CSN 誘導成多能幹細胞之多能性及表觀基因型之研究 (2012-2013)

從胃癌細胞 CS12 及胃黏膜細胞 CSN 導入轉錄因子 4F (Oct4, Sox2, c-Myc, Klf4)和 2F (Oct4, JDP2)以製備誘導型多能幹細胞並檢視其一系列的 HoxA 基因及幹細胞基因表現能力(結合子計畫一)。

目的二、由誘導多能性幹細胞製備癌症幹細胞 (CSCs) (2012-2014)

在培養誘導型多能幹細胞之培養液加入生長因子，例：BMP2、BMP6、BMP7、FGF5、FGF18、FGF19、TGFβ、Wnt5a、PDGF、IGF2 或突變的致癌基因，如：p53、kRas、APC 或能大量表現的 HoxA 基因以誘導表關基因改變進而產生癌症幹細胞。雖尚未有文獻證明胃癌癌症幹細胞標記為何，因此我們根據其他癌症類型挑選幾種可能的候選標記：CD133、CD44、CD24 等，並將注射細胞到免疫缺陷鼠以評估腫瘤生成能力（結合子計畫一、三、四、五）

目的三、利用 HoxA 家族基因與 kRAS 突變、腫瘤抑制基因 APC、p53 剔除以發展胃癌 (2012-2014)

在 kRas 突變及 p53 剔除或 kRas 突變、APC 和 p53 剔除的基因轉殖鼠體內導入 HoxA 基因以了解 HoxA 於誘導胃癌發生中所扮演的角色（結合子計畫三)。如同前述，我們將使用 HoxA 基因重組病毒或直接注射 CS12
、癌症幹細胞到基因轉殖鼠體內（結合子計畫一、三、四)。

目的四、誘導型多能幹細胞在胃癌發展中扮演的角色（2012-2014）

將誘導型多能幹細胞打入有 kRas 突變及 APC、p53 剔除的基因轉殖鼠體內觀察誘導型多能幹細胞是否阻礙或促進胃癌之發展（結合子計畫一、三、四)。另以體外實驗評估有無 HoxA 基因對 APC、kRas、p53 缺失的細胞影響。

目的五、誘導型多能幹細胞於活體及體外之分子影像實驗（2012-2014）

用紅外線螢光蛋白 (infrared fluorescent protein, IFP)和膽綠素系統 (biliverdin system)影像探討誘導型多能幹細胞或癌症幹細胞之 homing 及 trafficking 的能力。另一方面，以癌症幹細胞發展成癌症的各階段細胞用於胃癌藥物之篩選（結合子計畫四、五）

二、 實驗重要性

完成此份計畫可有幾項重要的發現：首先，我們將可以使用新的因子將病人胃癌細胞誘導成多能幹細胞；其次，發現從誘導型多能幹細胞得到之癌症幹細胞的表觀基因型、組蛋白與 DNA 甲基化的變異；第三，我們將找出胃癌中特定的致癌基因可能使誘導型多能幹細胞變

成癌症幹細胞；第四，找出在 APC、kRas 和 p53 等基因突變後，影響到新的下游目標基因如 HoxA 家族基因；最後，期望誘導型多能幹細胞對於胃癌治療是一個新的里程碑。

三、背景總述

自從 2006 年山中伸彌先生成功建立了老鼠的誘導型多能幹細胞 [1]，亦於隔年成功地發展出人類的誘導型多能幹細胞 [2, 3]，自此之後，世界各地的實驗室紛紛投入誘導型多能幹細胞的研究，到現在為止的發展已經足夠我們開始思考如何透過臨床前期的研究將誘導型多能幹細胞運用於再生醫學。第一株誘導型多能幹細胞是利用 Oct3/4、Sox2、Klf4、和 C-myc 四種遺傳因子混合後透過反轉錄病毒載體插入老鼠的纖維母細胞而產生 [1]，這株細胞與胚胎幹細胞一樣表現相似的特性，例如：無限制的生長能力，能夠分化為完整個體的所有細胞類型例如神經細胞、心肌細胞和其他細胞 [5, 6]，且誘導型多能幹細胞技術也被廣泛地認為具有相當大的潛力用於治療或其他醫學上的應用。以它們能夠分化成各種有功能的細胞為例，因此適合用於提供藥物篩選或毒理研究所需的純的實驗用細胞族群；同樣地，也可把從病人身體取得的細胞轉成誘導型多能幹細胞並用於發病機轉的研究及新一代治療藥物的發展 [7, 8]。

近期關於癌症幹細胞 (CSCs)具有自我更新能力並使腫瘤生成的多能特性之概念逐漸被提出 [9, 10]，並已有各種體外實驗及活體動物實驗證實癌症幹細胞擁有持續自我更新之潛能，因此，有假說認為惡性腫瘤是從具有不受控制且無限增生潛能和分化機制調節異常等特性的癌症幹細胞所衍生而來的，只是癌症幹細胞的起源至今仍未完整地了解 [9-11]。現有的其中一個論點認為癌症幹細胞是從已分化的細胞經由一些交替作用所產生的結果；另一論點則認為癌症幹細胞是由一些不成熟組織的幹細胞或祖先細胞發生腫瘤生成造成的結果，不論在哪個觀點中，基因的重新編碼用以調控腫瘤生成一直都是值得討論的議題 [9-11]。以腸癌為例，一連串的基因突變和表觀遺傳修飾的改變會導致連續性的傷害，進一步使惡性表型的表現加劇，一些例子如下：缺乏 polyposis coli (APC)會導致息肉增生；低度甲基化會產生管狀腺瘤；K-Ras 突變會生成管狀絨毛線瘤；大腸癌缺損基因 (DCC)導致絨毛腺瘤以及 p53 基因突變會產生腺癌等等 [12]。雖然胃癌的致病機轉上未被完整的釐清，但上述的例子或許都可被用於解釋胃癌的生成原因。

在此，我們著眼於以誘導型多能幹細胞來探討胃癌發生的機轉並找出胃癌發生的目標致癌因子。根據我們 microarray 及基因表現的初步研究顯示 HoxA 家族基因很有可能是造成胃癌腫瘤生成的目標基因 [13]，因此，我們提出 HoxA 家族基因及一些生長因子如 BMP、FGF 或 Wnt 可能參與胃癌發展的過程。此計畫將採用分子與細胞生物分析及基因轉殖鼠等試驗方法完成，且期望能夠更深入了解誘導型多能幹細胞於胃癌發展的新角色。

四、假說

比較從病人取得之胃上皮黏膜細胞 CSN 與胃癌細胞 CS12 之 DNA 微陣列及染色體製圖(chromosomal mapping)初步結果顯示 CS12 染色體 7P15.1-15.3 及 7P22.1-22.3 移位至第十二染色體上並大量表現 HoxA4、A5、A7、A9 及 A13 等 HoxA 家族基因 [13,14]，且發現用 siRNA 抑制 HoxA9 表現可預防胃癌發生，故提出假設認為 HoxA 基因可能是胃癌產生的重要致癌基因之一。再加上突變 p53、Kras 和 APC 等基因可會使癌症發生風險提高。因此，為證實此假說之正確性，欲完成以下實驗：(1)使用 4F (Oct4, Sox2, Klf4, c-Myc) 和 2F (Oct4、Jdp2)製備誘導型多能幹細胞;(2)從誘導型多能幹細胞中篩選出癌症幹細胞並確定其特性；(3)用 HoxA 家族基因及 APC、kRAS、p53 基因突變之交互作用誘使癌症幹細胞產生胃癌；(4)誘導型多能幹細胞在胃癌發展所扮演的新角色；(5)誘導型多能幹細胞及癌症幹細胞之影像系統探討細胞流向。

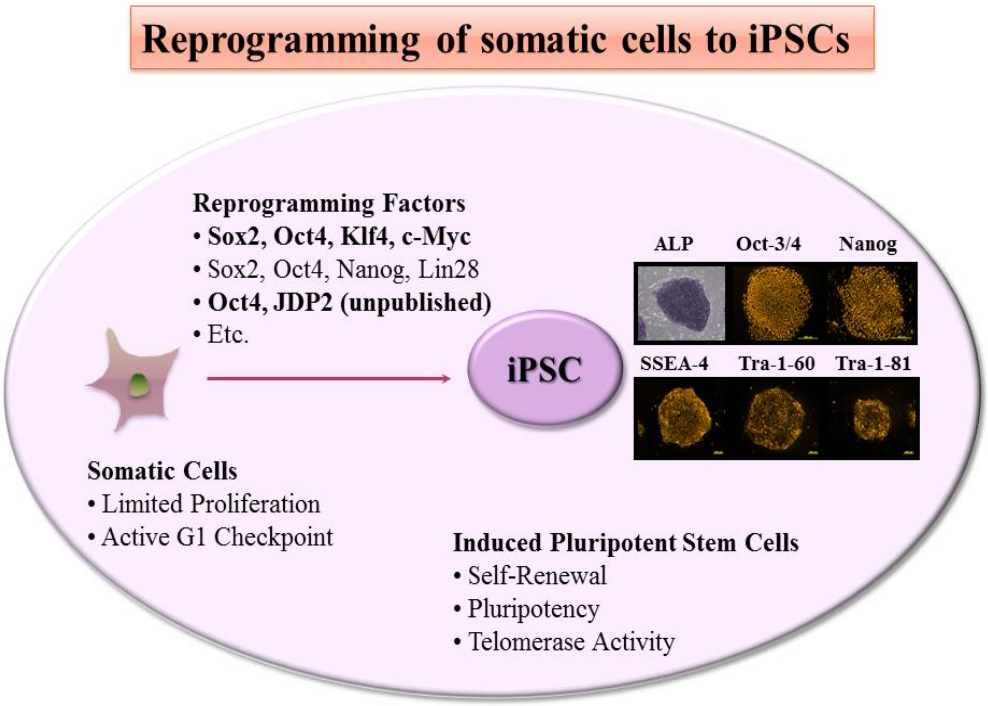

Figure 1. Schematic model of generation of iPSCs and CSCs derived from CSN and CS12 and iPSC/CSC related signal pathway.

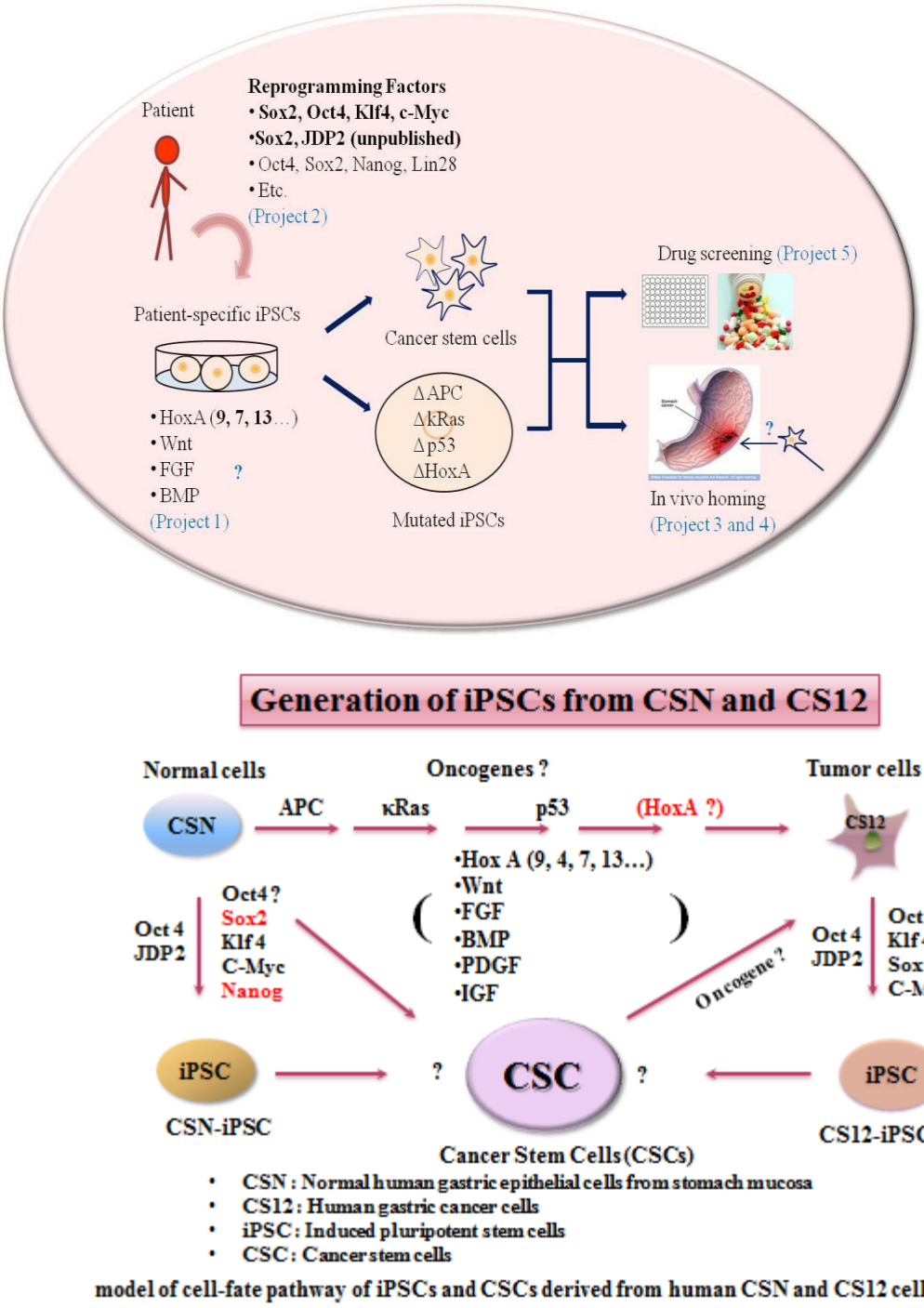

Figure 2. Schematic representation of generation of iPS cells from somatic cells and their characters and interrelation of iPSCs and CSCs for gastric cancer development.

五、實驗計畫

目標一、由胃癌細胞（CS12)及胃黏膜細胞（CSN)所得的誘導型多能幹細胞其多能性及表觀

基因型之探討

胚胎幹細胞/誘導型多能幹細胞的染色質中由不同的基因與表觀修飾以調控多能性，某些調控染色體轉錄的修飾酶，如：DNA 甲基轉移酶（DNA methyltransferases, DNMTs)、組蛋白甲基轉移酶(histone methyltransferases, HMTs)、組蛋白去甲基酶(histone demethylases, HDMCs)、組蛋白乙醯基轉移酶(histone acetyltransferases, HATs)、組蛋白去乙醯酶(histone deacetylases, HDACs)等，而這些染色質重組蛋白在胚胎幹細胞或誘導型多能幹細胞中扮演著調控多能性的重要角色。從初步實驗結果顯示由 Oct4 和 JDP2 可誘導體細胞（例：纖維母細胞)成誘導型多能幹細胞，儘管目前已有許多文獻闡述由四個因子所產生的誘導型多能幹細胞之機制及其優缺點，但 JDP2 引導的細胞核重新編碼機制仍有待釐清。例如 : JDP2 是否可取代 Sox2、Klf4、c-Myc 這些基因產生誘導型多能幹細胞？JDP2 與 Oct4 訊息如何互相調控？JDP2 對體細胞誘導型多能幹細胞及其分化細胞表基因的貢獻為何？H3K4me3 是否有能力產生全部胚層及所有細胞型態等等。目前，我們著重於 H3K27me3 和 H3K4me3 蛋白複合體（polycomb)的研究，並且與 PCR1、PCR2、TIP60/p400、核仁小體重組 NuRD 複合體、chromo domain helicase DNA-binding 1, CHD1、BRG1、DNA 甲基轉移酶（DNMT3a, 3b, DNMT3L)有關。從 JDP2 微陣列分析結果指出 JDP2 參與在 Wnt 訊息傳遞路徑中且作用於 secreted frizzled-related sequence protein 2, Srp2、Wnt1 inducible signaling pathway protein 2, Wisp2 及 Lymphoid enhancer binding factor 1/T cell-specific factor 4 (LEF1/TCF-4)…等目標蛋白。目前已知減少 p53 表現及缺氧環境可提高誘導型多能幹細胞產出率，因此，我們假設 JDP2-Wnt 及 Oct4 間可相互調控以活化誘導型多能幹細胞相關基因，而提高誘導型多能幹細胞之產出率。

(1) 結合 JDP2 訊號及 Oct4 可誘導核重組(nuclear priming)

用免疫組織化學分析確認鹼性磷酸酶（alkaline phosphatase)、SSEA4、SSEA5、Sox2、Oct4、Nanog 並用反轉錄 PCR 檢視其他重新編碼基因 LIF, STAT3, MEK, GSK3, Lin28, Fgf4 等的表現量。並以 DNA 甲基化實驗和 GenChip 微陣列比較體細胞、4F- (Oct4, Sox2, Klf4, c-Myc)和 2F-(Oct4, JDP2)之誘導型多能幹細胞間 Oct4 和 JDP2 啓動子活化程度。此實驗會跟陽明大學的徐明達教授和東京大學 Sumio Sugano 教授合作。另外，利用免疫化學染色確認纖維母細胞和 4F-或 2F-誘導型多能幹細胞染色體的改變，及動物實驗確認畸胎瘤分化成三個胚層的能力。

(2) 用 Chip-on-chip 陣列研究 JDP2 及 Oct4 表觀基因型

以 qPCR 比較胃上皮黏膜細胞跟 2F 誘導型多能幹細胞間蛋白複合體(polycomb)抑制 PCR1、PCR2、TIP60/p400、核仁小體重組 NuRD 複合體、chromo domain helicase DNA-binding 1, CHD1、BRG1、DNA 甲基轉移酶（例：DNMT3a, 3b, DNMT3L)之表現。以抗體偵測這兩株細胞間甲基化（H3K4me, H3K9me, H3K27me…)及乙醯化（H4K16Ac, H4K8Ac…)的表觀基因型改變, 特別是 H3K27me3 和 H3K4me3 已知與重新編碼修飾有關，故藉由基因組研究確認與 JDP2 和 Oct4 的相關性。

(3) Oct4 和 JDP2/Wnt 訊號互相影響可誘導 2F-誘導型多能幹細胞

為了瞭解 JDP2 在誘導 2F-誘導型多能幹細胞及幹細胞中所扮演的角色，會使用核轉移技術 (nuclear transplanatation technique)從 JDP2$^{-/-}$小鼠製備幹細胞並確認其 Oct4、Nanog、Klf4、c-Myc、MEK、GSK3、Lin28、Fgf4 基因表現量，而參予 Oct4 訊息傳遞路徑的 LIF, JAK, STAT3 和 Srp2, ß-Catenin, LEF-1/TCF4, TCF1 基因表現量亦會確認是否改變。

(4) 確認誘導型多能幹細胞的幹細胞型基因及 HoxA 家族基因之表現量

為了解 HoxA4、A5、A7、A9、A13 在 2F-誘導型多能幹細胞和癌症幹細胞間扮演的角色，欲比較原始癌細胞與誘導型多能幹細胞及其他胃癌細胞 AGS、N87、MKN45 間 HoxA 家族基因與幹細胞型基因之表現差異。

目標二、從誘導型多能幹細胞中產生癌症幹細胞

癌症幹細胞 (CSCs)是一群唯一支持腫瘤往惡性生長的細胞族群，又被稱為癌症創始細胞及癌症繁殖細胞 [15]。目前還沒有文獻指出有胃癌癌症幹細胞的存在，但有些報告指出透過 promoter-Cre construct 技術藉由篩選特定標記就能夠找出可疑的細胞。由於大部分的結腸直腸癌都是由 Wnt 訊息傳遞途徑的突變所造成，包括：負向回饋調控蛋白 APC 的缺失及 ß-catanin 的突變所造成活化，這兩項異常的結果都使得 Wnt 訊息傳遞途徑持續活化。有文獻指出從老鼠身上發現 apc 突變及 Lgr5 陽性幹細胞就是腸癌產生的起源 [16]，且此細胞亦具有 CD133 標記 [17]，另外從 Bmil-CreER knock-in 模型中發現 Wnt 訊息傳遞的失調對位於腺窩 (crypt)+4 或+5 位置的腸癌幹細胞也容易造成腫瘤產生 [18]，在胃的 Lgr5 陽性幹細胞族群可以視為由 Wnt 驅使腫瘤生成的細胞族群 [19-21]，儘管在不同癌症類型上有著非常大量的突變 但大部分的癌症原因都指向多種致癌基因與腫瘤抑制因子如PI3K、Myc、Ras、p53、p16^{Ink4a}和 RB 等。因此，我們想透過本實驗發展如何藉由增加一些生長因子如 BMP、FGF、Wnt 和一些突變致癌因子的小分子將誘導型多能幹細胞改變其表觀基因使轉變為癌症幹細胞。

(1) 從誘導型多能幹細胞中產生癌症幹細胞

為了鑑定從誘導型多能幹細胞中產生癌症幹細胞的培養條件，我們將嘗試在培養液加入某些生長因子如：BMP2、BMP6、BMP7、FGF5、FGF18、FGF19、TGFß、Wnt5a、PDGF、IGF2 或小分子以產生有胃癌癌症幹細胞標記 (CD133、CD44、CD24)的細胞。 [29-31]此外，我們會把細胞用於 APC、kRAS、p53 突變及 JDP2 剔除或 HoxA7、HoxA9、HoxA13 剔除的基因轉殖鼠上，從活體試驗的角度視其腫瘤生長的機率。

(2) 癌症幹細胞的多能性、癌化、及侵犯/轉移特性

一旦我們完成癌症幹細胞的建立，會比較 CS12 與 CSN 個別的癌症幹細胞與誘導型多能幹細胞兩者的幹細胞標記與癌症標記基因之表現情況，且進一步以 Chip on Chip 試驗比較兩者表觀基因 (如：組蛋白甲基化、乙醯基化和泛素化)的修飾情形以及 DNA 甲基化修飾，並完成癌化與侵犯/轉移試驗以確認其致癌能力。

目標三、HoxA 家族基因與突變或剔除致癌基因（APC、kRas、p53)對胃癌的發展

目前已可從文獻中得知 Hox 家族基因對於腫瘤發生或抗腫瘤發生非常重要 [22]，就 HoxA 家族基因與幹細胞而言，前述的 MLL/HoxA9 與 Bmil 的交互作用對於調控白血病的幹細胞老化是非常關鍵的 [23]，因此，我們想透過本實驗探討 HoxA 家族基因（A7、A9、A13）將會於 LSL-Kras;p53L/L 或 LSL-Kras;p53L/L;APCL/L 老鼠誘導胃癌發生，本項試驗會使用鄭光宏教授團隊的基因轉殖鼠為模型，一旦我們成功在此老鼠上產生腫瘤，我們將使用胺基酸突變後不產生功能的 HoxA7、A9、A13 或其 shRNA 以檢視對腫瘤產生的影響。此外，我們也欲探討 Wnt 訊息 (APC/β-catenin)與 HoxA 家族基因間的關係，以釐清 HoxA 基因如何與細胞週期之調控蛋白如 p53、$p16^{Ink4a}$ 及 kRas 進行交互作用。

(1) HoxA 家族基因與突變或剔除 APC、kRas 及 p53 對胃癌的發展

為了探討 HoxA 家族基因 HoxA4、A5、A7、A9、A13 在胃癌產生所扮演的角色，我們將以裸鼠或免疫缺陷鼠於小腸腔進行異體移植以分析腫瘤生長情形；或者於 LSL-Kras;p53L/L 或 LSL-Kras;p53L/L;APCL/L 老鼠接踵 HoxA 基因表現量較高的細胞，如：CS12 或 MKN45，以並評估老鼠的胃癌發展、癌症的轉移、存活率及 HoxA4、A5、A7、A9、A13 基因的表現量與是否產生突變，另外，我們也會製作經由突變使 HoxA 功能缺失的重組病毒或降低 HoxA 基因表現的 shRNA 用來檢驗胃癌的發生是否有減少以再次確認 HoxA 基因加強胃癌形成的能力，且以分子影像系統觀察在胃癌發展過程中誘導型多能幹細胞或癌症幹細胞的動向。

(2) HoxA 區域的表觀基因

癌症細胞、癌症幹細胞、誘導型多能幹細胞及原始細胞 CS12 和 CSN 的組蛋白及 DNA 動態改變將以測定組蛋白修飾的抗體（H3K4me3、H3K9me3、H3K36me3、H3K27me3、H4K16ac、H4K12ac、H4K8ac)和 APC、kRAS、P53 的抗體針對 HoxA 區域以 ChIP 試驗完成。

目標四、誘導型多能幹細胞於胃癌發展所扮演的角色

關於誘導型多能幹細胞有兩種可能性：其中一種是誘導型多能幹細胞在有利的特殊情況下會產生出如同癌症祖先細胞的癌症幹細胞，另一種可能性則是誘導型多能幹細胞會與體內特殊環境產生交互作用以抑制腫瘤的生長。然而，幹細胞生長的環境大大地影響著誘導型多能幹細胞的角色，因此，為了解誘導型多能幹細胞的作用，我們將移植誘導型多能幹細胞到動物模式上，並檢查其腫瘤或畸胎瘤在免疫缺陷鼠或裸鼠及基因轉殖鼠上的發展，此外，以導入 shRNA 的方式於誘導型多能幹細胞來再次確認 HoxA 家族基因所扮演的角色。

(1) 誘導型多能幹細胞對胃癌發展的影響

將誘導型多能幹細胞透過尾靜脈注射或腹腔注射到 kRas 突變、APC 及 p53 剔除的基因轉殖鼠視其胃癌發展的效率，也會把誘導型多能幹細胞異體移植至 LSL-kRAS;p53L/L 或 LSL-kRas;p53L/L;APCL/L 老鼠的實驗，並探討老鼠的存活率與腫瘤生長情況，另外，誘導

型多能幹細胞的轉移能力也會與一般胃癌細胞 CS12、AGS、N87、MKN45 相互比較。

(2) 探討誘導型多能幹細胞對 HoxA 表觀基因之改變

本實驗將探討幹細胞基因及 HoxA 之表觀基因修飾情況以確認 HoxA 基因所扮演的角色，並用 Chip-on-chip 分析受 Bach2 誘導的組蛋白甲基酶及 DNA 甲基酶 DNMT3a 是否受 HoxA 基因的調控，以及在胃癌細胞中，上述基因是否受誘導型多能幹細胞影響其組蛋白和 DNA 的甲基化程度。

目標五、活體及體外誘導型多能幹細胞之分子影像分析

誘導型多能幹細胞與癌症幹細胞在體內如何 homing 是個熱門的議題 利用紅外線螢光蛋白 (infrared fluorescent protein, IFP)和膽綠素系統 (biliverdin system)標定 CS12 (HoxA 表現量高)和 CSN (對照組)及各自的誘導型多能幹細胞及癌症幹細胞以比較各別 homing 能力，胃癌細胞的副群 (side population)可能包含具癌症幹細胞特質的細胞群，再使用 Lgr5、CD133、CD44、CD24 及 Wnt 蛋白作為癌症幹細胞標記 (結合子計畫三)。一般來說，組織、幹細胞及受損程度會決定細胞的移動、分化及生長，受傷的組織會分泌因子誘使癌症幹細胞和誘導型多能幹細胞 homing。基底細胞、胞外間質、循環性生長因子、循環性分化因子會決定幹細胞基因活化及功能，諸如往特定方向移動、分化成特定細胞或靜止在特定位置，這些因子可改變幹細胞基因的表現型態，在此，我們欲使用分子影像系統作為偵測。

(1) 標記誘導型多能幹細胞與癌症幹細胞

在誘導型多能幹細胞與癌症幹細胞標記紅外線螢光蛋白 (IFP)和膽綠素 (biliverdin system)。

(2) 追蹤誘導型多能幹細胞與癌症幹細胞在基因轉殖鼠體內的動向

利用已被標記的誘導型多能幹細胞與癌症幹細胞觀測 homing 及癌症發展進程。

(3) 在基因轉殖鼠體內偵測 HoxA 家族基因與胃癌幹細胞標記

將製備抑制或大量表現 HoxA 基因的重組病毒，CD133、CD44、CD24 等胃癌幹細胞標誌的啓動子 (Promoter)也將與螢光基因融合以便於追蹤實驗之運用。

(4) 以誘導型多能幹細胞與癌症幹細胞進行篩選藥物

以誘導型多能幹細胞與癌症幹細胞進行新藥物之篩選，確認 JNK、ERK 路徑訊息傳遞情形，而新藥將可被用於預防胃癌的發展。

Title: The role of transcription factor JDP2 in cell cycle control, senescence and oncogenesis

(Background)

We have identified the transcription factor, Jun dimerization protein 2 (JDP2), which is a member of the AP-1 family. We have found that JDP2 is an AP-1 repressor that controls cell growth, cell differentiation and replicative senescence induced by oxidative stress. These multiple functions of JDP2 are determined by the DNA-binding domain and the domain of inhibition of histone acetylation (INHAT). Moreover, JDP2 plays a critical role in cell cycle arrest through regulated expression of cyclin A2, cycling E2 and $p16^{Ink4a}$, which are involved with the $p19^{Arf}$-Mdm2-p53-p21-cyclin/cycling-dependent kinase (CDK) and $p16^{Ink4a}$-cycling/CDK-Rb-E2F networks. Therefore, this proposal is aimed at exploring the role of JDP2 in antioxidant production, and reactive oxygen species (ROS) regulation. Molecular oxygen is essential for the survival of almost all eukaryotes. Under normal physiological conditions, RO-including hydrogen peroxide, superoxide, peroxynitrite, and hydroxyl radical, are generated as metabolic by-products. However, increased levels of ROS can lead to oxidative stress and cell injury. In general, mammalians have developed a variety of inducible genetic programs to adapt to the presence of ROS. As a first cellular reaction in response to oxidative/electrophilic stress, an array of defense genes is activated, which, in most instances, leads to the neutralization of oxidative stress, its effects, and finally to survival. In the absence of appropriate defense mechanisms, the accumulation of ROS and electrophiles can lead to membrane and DNA damage, mutagenicity, degeneration of tissues, premature aging, apoptotic cell death, cellular transformation, and cancer (Cancer Res 57, 2979-2985, 1997). Enzymes with antioxidant capabilities capable of inactivating ROS and preventing ROS-initiated reactions include superoxide dismutases, catalase, and glutathione peroxidase and belong to the group of "direct" antioxidants. In contrast, phase II detoxifying (conjugating) enzymes are classified as "indirect" antioxidants based upon their role in maintaining redox balance and thiol homeostasis which include glutathione *S*-transferase isozymes and NADP(H):quinine oxidoreductase (NQO1), γ-glutamyl cysteine synthethase, and UDP-glucronosyltransferase (USTs). They contribute to biosynthesis and the recycling of thiols or facilitate the excretion of oxidized, reactive secondary metabolites (quinines, epoxides, aldehydes, and peroxides) through reduction/conjugation reactions during the process of xenobiotic detoxification (Adv Enzyme Regul 44, 335-367, 2004).

The expression of several enzymes responsible for these phase II reactions, such as various glutathione S-transferases and UDP-glucuronosyltransferases, are also regulated in an AhR-ARNT-dependent manner. In addition, these phase II enzymes are transcriptionally co-regulated by antioxidant-responsive elements (AREs; 5'-G/ATGACNNNGC-3') located adjacent to the xenobiotic-responsive elements (XRE). These AREs are recognized by the transcription factor

like nuclear factor-erythroid 2-related factor 2 (Nrf2), the master regulator of the cellular antioxidant response. In the cytoplasm Nrf2 is bound to kelch-like ECH-associated protein 1 (Keap1), which prohibits Nrf2 nuclear translocation and thus facilitates the degradation by proteosome. Upon oxidative stress, dissociation of Nrf2 from Keap1 permits Nrf2 shuttling into the nucleus, where it binds to small Maf proteins (MafK, MafF and MafG) to form a transcriptionally active complex to induce ARE-dependent responses (Free Radic Biol Med 47, 1304-1309, 2009). Because exposure to AhR ligands such as dioxins, polycyclic aromatic hydrocarbons, and flavonoids results in the CYP-mediated formation of reactive oxygen species (ROS) and electrophilic metabolites, the interaction between AhR and Nrf2 signaling is probably a crucial enhancer of protection against toxic by-products of the AhR-dependent detoxification process. The dissociation of Nrf2 from Keap1 permits Nrf2 shuttling into the nucleus, where it binds to small Maf proteins (MafK, MafF and MafG) to form a transcriptionally active complex to induce ARE-dependent responses (Free Radic Biol Med 47, 1304-1309, 2009). Because exposure to AhR ligands such as dioxins, polycyclic aromatic hydrocarbons, and flavonoids results in the CYP-mediated formation of reactive oxygen species (ROS) and electrophilic metabolites, the interaction between AhR and Nrf2 signaling is probably a crucial enhancer of protection against toxic by-products of the AhR-dependent detoxification process. Apart from the small Maf proteins, other bZIP factors, such as JunD, PMF-1, and ATF4, bind to ARE and have the ability to regulate ARE-driven transcription (Gene 294, 1-12. 2002; Science 300, 2097-2101, 2003). Moreover, the small Maf proteins are able to not only dimerize with CNC factors, such as Nrf2, but also with other bZIP factors, including Fos, FosB, Bach 1, and Bach 2, via their leucine zipper domain (J. Mol. Biol. 376, 913-925, 2008) because JDP2 is also a member of the bZIP family of transcription factors, we examined whether JDP2 binds to Maf-family and/or Nrf2 proteins, and whether it is able to regulate ARE–dependent genes encoding antioxidant and detoxification enzymes.

Here we report that JDP2 indeed associated with ARE and acted as a novel key cofactor of the Nrf2/MafK complex to regulate ARE-mediated gene expression and ROS production. Our results provide evidence that JDP2 plays a critical role in the cellular adaptive response to ROS and electrophiles generated by cellular stimuli. This year's work is focused on subproject 2.

2. The role of JDP2 in replicative senescence

Conduct a study on the mechanisms underlying the oxygen-induced expression of JDP2 and the induction of $p16^{Ink4a}$ and $p19^{Arf}$ by JDP2 to induce replicative senescence.

We are now submitting these results as described below and now it will be revised in Nucleic Acids Research.

The progress reports of other subprojects are summarized as below.

1. The role of JDP2 in cell cycle control

Conduct a study of the transcriptional and epigenetic control of JDP2 in networks of $p16^{Ink4a}$-cyclin/CDK-Rb-E2F and $p19^{Arf}$-Mdm2-p53-p21-cyclin/CDK to induce the cell cycle arrest (see **Figure 1**).

We have quantitated the expression of JDP2 target genes using qPCR analysis in the case of WT and JDP2 KO MEFs. This indicates that some of JDP2 targets are involved in Wnt signal (unpublished; see **Figure 2**).

4. The role of JDP2 in tumorigenicity

Identify the role of the tumor suppressor activity of JDP2 using $JDP2^{-/-}p53^{-/-}$ double knockout mice as well as determine the potential therapeutic activity of JDP2 and its derivative and prepare a mouse model of medulloblastoma. We have now prepared the double KO mice and some of them caused the malformation of skull. Now we will examine the cerebellum of brain.

Methods:

Transfection of siRNAs

Predesigned siRNAs against human/mouse/rat Nrf2 (S9492: sense, 5′–CGUUUGUAGAUGACAAUGAtt–3′; antisense, 5′–UCAUUGUCAUCUACAAACGgg–3′) and human/mouse/rat MafK (S194859: sense, 5′–GCAGACUCUCGACAUCCGAtt–3′; antisense, 5′–UCGGAUGUCGAGAGUCUGCat–3′) and a control scrambled siRNA (ID; 4611) were purchased from Ambion (Austin, TX, USA). The siRNA against Jdp2 (GFP control, TRCN 0000081973, 0000081974, 0000081976 and 0000081977) was synthesized by Nippon EGT (Toyama, Japan) according to the Gene Swatter siRNA program. The sequence of the JDP2 siRNA is available from the authors upon request.

Analysis of 8-oxo-dGuo, glutathione and cellular ROS

8-Oxo-dGuo and glutathione were measured using liquid chromatography/mass spectrometry, as described elsewhere (Rapid Comm Mass Spec 22, 432-440, 2008). To measure the net intracellular accumulation of ROS, a fluorescent probe species (2′, 7′-dichlorofluorescein, DCF-DA; Molecular Probes, Eugene, OR, USA) was used. After 2 h of treatment with TPA, cells were washed twice with HBSS solution (GIBCO, Carlsbad, CA, USA) and loaded with 10 mmol/L of DCF-DA in a 5% CO2 incubator kept at 37℃. After 30 min, cells were washed twice with HBSS (GIBCO), suspended in complete medium, and examined under a microscope or flow cytometry. The number of DCF-stained cells was calculated in an area of 8.75 mm^2.

Transient transfection and luciferase reporter assay

The activities of luciferase and renilla were measured as described elsewhere (Oncogene 29, 6245-6556, 2010). WT and *Jdp2* KO MEFs (1×10^5 cells) were plated into each well of 12-well plates and cultured for 24 h. The cells were then cotransfected with indicated amount of pGL2-hQR41-firefly luciferase reporter and pGL4.74-TK plasmid encoding renilla luciferase (Promega) in the presence or absence of pcDNA3 encoding Nrf2, MafK or Jdp2 using the Effectene transfection reagent kit (Qiagen). After 24 h of incubation, the cells were incubated in the presence or absence of 10^{-6} M TPA or 10 μM sulforaphane in 0.1% DMSO (or 0.1% DMSO alone, as a control) for 24 h.

Immunoprecipitation and Western blot analysis

Cells were harvested using a modified RIPA buffer (10 mM Tris-HCl, pH 8.0, 150 mM NaCl, 1 mM EDTA, 0.1% NP-40, 1% deoxycholate, 50 mM sodium fluoride, 50 mM sodium orthovanadate, and 1 mM PMSF) and a protease inhibitor cocktail (Nacalai Tesque, Kyoto, Japan). The preparation of cell lysates, SDS-PAGE (8 or 10% Gel) and Western blotting were carried out as described elsewhere (Mol Cell Biol 22, 4815-4826, 2002).

Protein–protein interaction assay

A rabbit reticulocyte lysate system (Promega, Madison, WI, USA) was used to prepare the recombinant proteins of Nrf2, MafK, and JDP2, according to the manufacturer's protocol. GST and GTS-fusion proteins of GST–Nrf2, GST–MafK, and their deletion mutants were prepared as described in Supplementary Methods. For protein–protein interaction assays, 10 μL of glutathione-sepharose beads containing 10 μg of GST–fusion proteins were incubated with 5 μL of nonradioactive *in vitro*-translated proteins in a final volume of 500 μL of binding buffer. After incubation for 2 h at 4℃, the bead-bound protein complexes were washed extensively (five times) with wash buffer [100 mM NaCl, 20 mM 4-(2-hydroxyethyl)-1-piperazineethanesulfonic acid (HEPES), pH 7.9, 0.1% NP-40, 5 mM $MgCl_2$, and 0.5 mM PMSF], followed by elution of protein complexes with SDS sample buffer and loading onto 8 or 15% SDS-PAGE. The proteins bound to GST-fusion proteins were visualized by Western blotting using Nrf2-, MafK-, or JDP2-antibodies.

EMSA

Five micrograms of GST fusion protein or 10 ng of *in vitro* translated proteins were incubated at 25°C for 30 min with T4-kinased NQO1-ARE oligonucleotide (5′–CAGTCACAGTGACTCAGCAGAATCT–3′) in the presence or absence of unlabeled double-stranded mutant AREs (Supplementary Table S1). The products were resolved at 4℃ on a 5% nondenaturing polyacrylamide gel in 0.5 × Tris-Borate/EDTA buffer and exposed to a radioactive imaging plate, and detected on an FLA-2000 machine (Fuji Photo Film, Tokyo, Japan) as

described elsewhere (Free Redic Biol Med 42, 1690-1703, 2007).

ChIP assay

ChIP assays were performed as described by Kotake *et al.* (Gene Dev 21, 49-54, 2007), with modification of the washing conditions. The immunoprecipitated protein–DNA complexes were washed twice with binding buffer (10 mM HEPES, pH 7.9, 10 mM Tris-HCl, pH 7.9, 12.5% glycerol, 0.25% NP-40, 0.5% Triton X-100, 0.24 M NaCl, 0.75 mM MgCl2, 1.1 mM EDTA, and protease inhibitor mixture) and then washed twice with Tris/EDTA buffer (10 mM Tris-HCl, pH 7.9, 1 mM EDTA). The protein–DNA complexes were disrupted with proteinase K (Sigma-Aldrich) at pH 6.8. DNA was extracted with phenol and chloroform, precipitated in ethanol, and analyzed by real-time PCR using the Power SYBR® Green Master Mix and the primers shown in Supplementary Table S2.

Immunofluorescence

Cells were cultured in Iscove's modified Dulbecco's medium containing 1% BSA and 4% bovine serum at 37 ^{o}C. After *in situ* extraction with 0.1% Triton X-100 at 4 ^{o}C for 3 min, cells were fixed in 4% paraformaldehyde for 20 min and permeabilized in PBS containing 0.1% saponin and 3% BSA at room temperature (Exp Cell Res 315, 1117-1141, 2009). Cells were stained with anti-JDP2 (#249) and anti-Nrf2 (Santa Cruz Biotechnology) or anti- MafK (Santa Cruz Biotechnology) antibodies for 2 h, washed with PBS containing 0.1% saponin, and stained with Alexa Fluor 488- or Alexa Fluor 546-conjugated secondary antibodies for 1 h. For DNA staining, cells were treated with 200 μg/mL RNase A for 30 min and 25 ng/mL TOPRO-3 for 30 min. Stained cells were mounted with antifade reagent. Confocal and Nomarski differential-interference contrast images were obtained using an FV500 laser-scanning microscope (Olympus) as described previously (Oncogene 29, 6245-6256, 2010).

TPA-induced epidermal thickening *in vivo*

Epidermal thickening was measured as described previously (Oncogene 29, 6245-6256, 2010). Briefly, the dorsal skin of each mouse (six pairs of WT and KO mice) was painted with TPA twice at an interval of 24 h (8.1 nmol in 100 μL acetone; Sigma-Aldrich), or painted with sulforaphane (15 nmol in 100 μL acetone; Sigma-Aldrich), which was topically applied. Mouse skin was collected 1 h after the second TPA treatment or sulforanphane treatment. The tissues were fixed with 4% paraformaldehyde, embedded in paraffin, and sectioned at a thickness of 5 μm. The epidermal thickness of the skin was measured at 10 sites of a randomly selected region using an Olympus microscope (Olympus, Tokyo, Japan). The vertical thickness of the epidermis was defined as the distance from the stratum basal to the stratum corneum. All mice were housed at the National

Laboratory Animal Center mouse facilities in accordance with the Institutional Animal Care and Use Committee.

Transient transfection and luciferase reporter assay

The double stranded oligonucleotides corresponding to human *NQO1* gene ARE (–471 nt to –447 nt) was synthesized with *Bgl*II/*Kpn*I linker, and annealed, phosphorylated by T4 polynucleotide kinase, and cloned into pGL4.10 vector to generate reporter plasmids pGL4-hARE25-luciferase. A pGL2-hQR41-luciferase reporter plasmid containing the 25 bp ARE of the human *NQO1* gene was kindly gifted from Dr. Jeffrey A. Johnson (University of Wisconsin, Madison, WI, USA) (Mol Cell Biol, 26, 3773-3784, 2006). WT and *Jdp2* KO MEFs (1×10^5 cells) were plated into each well of 12-well plates and cultured for 24 h. The cells were then cotransfected with 100 ng of an ARE plasmid encoding firefly luciferase and 50 ng of the pGL4.74-TK plasmid encoding renilla luciferase (Promega) using the Effectene transfection reagent kit (Qiagen) as described in the manufacturer's protocol. For overexpression, cells were cotransfected with pcDNA3 encoding Nrf2, MafK, or Jdp2. The total amount of transfected DNA was kept constant at 1 μg/well by the addition of a pcDNA3 control vector. After 24 h of incubation, the cells were incubated in the presence or absence of 10^{-6} M TPA or 10 μM sulforaphane in 0.1% DMSO (or 0.1% DMSO alone, as a control) for 24 h. The activities of luciferase and renilla were measured in a luminometer (Berthold Technologies Gmbh and Co. KG, Bad Wildbad, Germany) using the Dual-Luciferase Reporter Assay System (Promega, Madison, WI, USA) as described elsewhere (Oncogene 29, 6245-6256, 2010). Luciferase activity values were normalized to transfection efficiency, which was monitored by renilla expression, and ARE transcription activity was expressed as fold induction relative to that of the control cells.

Immunoprecipitation and Western blot analysis

Cells were harvested using a modified RIPA buffer (10 mM Tris-HCl, pH 8.0, 150 mM NaCl, 1 mM EDTA, 0.1% NP-40, 1% deoxycholate, 50 mM sodium fluoride, 50 mM sodium orthovanadate, and 1 mM PMSF) and a protease inhibitor cocktail (Nacalai Tesque, Kyoto, Japan). The lysates were homogenized twice (10 s each time) in an ultrasonicator and incubated on ice for 30 min. The homogenates were centrifuged at 14,000×g for 15 min at 4°C. The supernatants were collected and protein concentration was determined using a protein assay kit (Bio-Rad Laboratories, Hercules, CA, USA). Each supernatant was incubated with JDP2-specific antibody and then incubated with beads of protein A/G-sepharose (Amersham Pharmacia Biotech, Uppsala, Sweden). The beads were pelleted, washed, and applied to Western blotting. Whole-cell lysates (40 μg of protein) or immunoprecipitates were run on 8 or 10% SDS-PAGE and transferred onto PVDF membranes (Amersham Pharmacia Biotech). After blotting, the membranes were incubated with specific antibodies overnight at 4°C, followed by further incubation for 1 h with an HRP-conjugated secondary antibody. Bound antibodies were detected using an ECL system and the relative amount

of proteins associated with specific antibodies was quantified, using the Lumi Vision Imager software (TAITEC, Saitama, Japan).

Electrophoretic mobility shift assay (EMSA)

Electrophoretic mobility shift assay (EMSA) was performed as described elsewhere (Mol Cell Biol 22, 4815-4826, 2002). The 5′-end labeling of the NQO1-ARE oligonucleotide (5′-CAGTCACAGTGACTCAGCAGAATCT-3′) was performed using T4 polynucleotide kinase (Takara, Shiga, Japan) with 10 pmol of double-stranded oligonucleotide and 50 μCi of [γ-^{32}P]ATP (5000 Ci/mmol; Amersham Biosciences, Buckinghamshire, UK). The labeled oligonucleotides were purified on a SephadexG-25 spin column (Amersham Biosciences). Five microgram of GST-fusion protein and 10 ng of *in vitro* translated proteins were incubated at 25°C for 30 min with labeled or unlabeled competitor oligonucleotides in binding buffer [25 mM Tris-HCl, pH 7.5, 75 mM KCl, 0.3% NP-40, 7.5% glycerol, 2.5 mM DTT, 1 mg/mL BSA and 1 μg of poly(dI)· poly(dC)]. The specificity of binding was assessed by competition with excess unlabeled double-stranded mutant AREs (Supplementary Table S1). The products were resolved at 4℃ on a 5% nondenaturing polyacrylamide gel in 0.5 × Tris-borate/EDTA buffer. After electrophoresis, the gel was dried on 3 MM chromatography paper (Whatman, Maidstone, UK), and exposed to a radioactive imaging plate, and then detected on an FLA-2000 machine (Fuji Photo Film, Tokyo, Japan).

III. Results

JDP2 reduces the TPA-mediated production of ROS and enhances antioxidant activity

The level of ROS is tightly controlled by an inducible antioxidant program that responds to cellular stressors and is regulated predominantly by Nrf2 and its repressor protein, the kelch-like ECH-associated protein 1 (Keap 1) (Gene 294, 1-12. 2002; Science 300, 2097-2101, 2003; Free Redic Biol Med 42, 1690-1703, 2007). In contrast to the acute response of Nrf2, in the steady state, some somatic mutations cause destabilization of Nrf2 and decrease the constitutive transcription of its target genes, indicating that enhanced ROS detoxification and additional Nrf2 functions may be critical for the induction of the antioxidant response (Trends Biochem Sci 34, 176-188, 2009). Because JDP2 is a member of the stress-induced AP-1 protein family (Mol cell Biol 17, 3094-3102, 1997), we examined the role of JDP2 in ROS production and antioxidant response. Strikingly, *Jdp2* KO MEFs exhibited about 1.9-fold higher basal levels of ROS than WT MEFs, and TPA treatment led to higher levels of ROS in *Jdp2* KO versus WT MEFs (**Figure 3**). As expected, exposure of MEFs to the ROS inhibitor CO-releasing molecule tricarbonyl dichlororuthenium (CORM)

abolished the TPA-induced increase in ROS production. We conclude that deletion of JDP2 leads to higher basal as well as TPA-induced levels of ROS, and thus JDP2 function is required to keep ROS levels low. Because ROS alterations can affect the intracellular redox state (J Biol Chem 275, 15466-15473, 2000), we next measured the ratio of reduced to oxidized glutathione (GSH/GSSG) in WT and *Jdp2* KO MEFs. While the level of total glutathione was enhanced by 1.6-fold in *Jdp2* KO MEFs compared with WT MEFs in the absence or presence of TPA (**Figure 3**), the GSH/GSSG ratio was reduced by about 55% in the presence of TPA, thus promoting a more reduced intracellular environment (Figure 1C). Moreover, the level of 7, 8-dihydro-8-oxo 2'-deoxyguanosine (8-oxo-dGuo), which is one of the major products of DNA oxidation, increased by 1.3-fold in *Jdp2* KO MEFs compared with WT MEFs, and TPA induced the production of 8-oxo-dGuo by 1.5-fold in WT MEFs and 2.1-fold in *Jdp2* KO MEFs (**Figure 3**). Thus, compared with WT MEFs, the levels of ROS, 8-oxo-dGuo, and total glutathione were increased, whereas the GSH/GSSG ratio was decreased in *Jdp2* KO MEFs, either left untreated or exposed to TPA. These results again support the notion that JDP2 function is required to keep ROS levels in check.

JDP2 is involved in TPA-mediated ARE transactivation

The increased ROS levels in *Jdp2* KO MEFs suggest that some of the enzymes involved in keeping ROS levels under control may not be produced at KO-typed levels. Indeed, an immunoblot surveying several of the key components in fighting ROS levels revealed that basal levels of the HO-1 protein were 5-fold lower in *Jdp2* KO MEFs than in WT MEFs (**Figure 4**). The level of expression of Nrf2 was almost the same, while the level of MafK was 3-fold higher in *Jdp2* KO MEFs compared with WT MEFs (**Figure 4**). We conclude that lower HO-1 protein levels may in part explain the increased levels of ROS in JDP-2 KO MEFs cells.

Since Nrf2 acts as the key transcription factor in triggering ROS-induced gene expression, we investigated Nrf2 activity in JDP2 KO MEFs. An ARE driven luciferase reporter plasmid was transfected into WT and *Jdp2* KO MEFs together with increasing amounts of Nrf2. Nrf2 enhanced ARE promoter activity in WT MEFs, but failed to do so in *Jdp2* KO MEFs (**Figure 4**). Similarly, TPA stimulated ARE–luciferase activity 3-fold in WT MEFs after 24 h, while essentially no stimulation was observed in JDP2 KO MEFs (**Figure 4**). As expected, the ROS inhibitor CORM led to the complete inhibition of the TPA-induced ARE activity (**Figure 4**). These results indicate that ectopic Nrf2 activity is severely impaired by the absence of JDP2.

We next tried to rescue Nrf2-mediated transactivation in *Jdp2* KO MEFs by co-transfecting a JDP2 expression plasmid together with Nrf2 at the optimal dose (50 ng; **Figure 4**). We found that JDP2 influenced Nrf2-mediated ARE promoter activity in a dose-dependent manner, slightly repressing at a lower dose and stimulating at a higher dose. Thus, a partial rescue was observed by re-expressing JDP2 at a higher dose in the KO MEFs. Of note, the biphasic response to increasing

levels of JDP2 was also observed in HepG2 cells. JDP2 exhibited a repressor function at a lower dose, but acted as a positive regulator at a higher dose in these cells (data not shown). The molecular mechanism underlying this biphasic pattern of ARE reporter activity induced by JDP2 remains to be determined.

To complement these experiments, we used siRNAs to knock down (KD) the expression of Nrf2 and JDP2 in WT MEFs. The ARE reporter gene activity was decreased by 26–28% after Nrf2 KD and by 46–65% after JDP2 KD in WT MEFs in the absence and presence of TPA, respectively (unpublished). Similarly, the expression of ARE–luciferase was decreased by 10-35% after Nrf2 KD in *Jdp2* KO MEFs. However, expression of the reporter gene was unaffected in the negative control (nonspecific random siRNA; NS). Each siRNA reduced the expression of the respective endogenous Nrf2 and JDP2 proteins, but the control siRNA did not (unplublished). Thus, all these results are consistent with the view that JDP2 function is critical for Nrf2 to efficiently enhance ARE-dependent transcription.

Effect of JDP2 on sulforaphane-induced ARE-luciferase activity and epidermal thickness

Sulforaphane (SFN) is a potent inducer of phase II detoxification enzymes and inhibits tumorigenesis in animal models (Cancer Res 60, 1426-1433, 2000; Cell Mol Life Sci, 64, 1105-1127, 2007). To determine whether JDP2 is involved in SFN-induced ARE transactivation, we transfected an ARE–luciferase plasmid into both WT and *Jdp2* KO MEFs and treated the cells for 12 h with 10 μM SNF. In the absence of SNF, the ARE activity of *Jdp2* KO MEFs was reduced by about 50% relative to that of WT MEFs, which is similar to the results shown in Figure 2. SNF enhanced ARE transcription by 2.5-fold in WT MEFs and by 3.75-fold in *Jdp2* KO MEFs; however, both activities were reduced by 70% in the absence of SNF in *Jdp2* KO MEFs (unpublished). The expression of the Nrf2 protein in WT and *Jdp2* KO MEFs was increased by 2.5–3.6-fold in response to SFN, but the level of the MafK protein was not affected by SFN in WT or *Jdp2* KO MEFs (unpublished). However, the level of MafK in the absence of SFN was 2.5-fold higher in *Jdp2* KO MEFs compared with WT MEFs.

To investigate whether ROS production is critical for TPA-induced epidermal thickening in *Jdp2* KO mice *in vivo*, we compared the skin of TPA-treated WT and *Jdp2* KO mice in the presence or absence of pretreatment with SFN. The epidermal thickness of the hairless skin from *Jdp2* KO mice was increased by about 1.7-fold after TPA treatment compared with that of WT mice (unpublished). Administration of SFN to WT mice had only a limited effect on epidermal thickening, whereas administration of SFN to *Jdp2* KO mice induced a significant epidermal thickening, although this increase in epidermal thickening was about half of that induced by TPA (unpublished). Similarly, the formation of colonies by mouse embryonic fibroblasts from *Jdp2* null mice (*Jdp2* KO MEFs) was increased by about 2.9–3.7-fold compared with those of wild-type mouse MEFs (WT

MEFs) in the absence or presence of TPA (unpublished). Taken together, these data suggest that JDP2 antagonizes TPA-dependent cell proliferation *in vivo* in the epidermis and *in vitro* in MEFs.

The zipper region of JDP2 is required for its association with ARE *in vitro*

We performed an electrophoresis mobility shift assay (EMSA) to examine whether JDP2 binds to an ARE-containing DNA fragment. To identify the domain of JDP2 that is involved in ARE binding, we used a series of deletion mutants of JDP2 and examined their binding to ARE (unpublished) using a [^{32}P]-labeled ARE probe (unpublished). Jdp2 mutant proteins without basic and bZIP domains (NT70) did not bind to ARE. Moreover, neither the mutant with a basic domain alone (NT102) nor the ZIP mutant (FL34R) bound to ARE. These data indicate that the zipper domain of JDP2 is critical for binding to the ARE–DNA core; in particular, the leucine residues located at positions 114 and 121 were critical for the process.

Cooperation of JDP2, MafK, and Nrf2 proteins toward ARE binding

To study the reciprocal interactions of JDP2, MafK, and Nrf2 *in vitro*, we examined the activity of heterodimer formation using each recombinant GST-protein and protein synthesized by *in vitro* transcription and translation system (IVT-protein). We found that the bZIP domain and the basic domain of JDP2 are required for the interaction with MafK and Nrf2 protein, respectively (unpublished). We also prepared a series of deletion mutants of GST-MafK and GST-Nrf2, and examined their interaction. The DNA-binding domain of MafK and the C-terminal region containing the half-bZIP region of Nrf2 are sufficient for interaction with JDP2 (unpublished). Moreover, the C-terminal region containing the zipper region and CHR region of MafK is critical for the interaction with Nrf2 (unpublished). Our data revealed that both JDP2 and MafK bound to ARE and both were able to interact subsequently with Nrf2. These data suggest that the complex (JDP2/ MafK/Nrf2) exists and plays a critical role in ARE-mediated transcription. To test this, we prepared *in vitro*-translated Nrf2, MafK, and Jdp2 proteins. Nrf2 did not bind to ARE; in contrast, both MafK and Jdp2 bound to ARE, probably via their homodimerized forms. Jdp2 exhibited increased binding to ARE in the presence of Nrf2 or MafK or both, in a dose-dependent manner. Nrf2 also showed dose-dependent binding to ARE in the presence of MafK or Jdp2 and MafK. Moreover, MafK exhibited dose-dependent binding to ARE in the presence of Jdp2.

Next we studied the DNA-binding elements that are responsible for the regulation of the oxidative-stress-induced gene NQO1 mediated by the JDP2/MafK/Nrf2 complex. A series of deletion mutants corresponding to the AP-1-like element, ARE core, and GC box motifs were constructed derived from the NQO1 gene (Free Radic Biol Med 47, 1304-1309, 2009) and EMSA using recombinant Jdp2 and MafK proteins was performed (unpublished). The cold competitors of ARE core plus GC box (M1), AP-l-like plus ARE core (M3), ARE core alone (M5), and WT

blocked the binding of Jdp2, whereas cold competitors of AP-1-like plus GC box (M2), AP-1-like (M4), GC box (M6) and M7 did not compete with the binding of Jdp2 (unpublished). These data Competitive DNA-binding assay demonstrated that JDP2 binds the ARE core (TGACTCA) of the ARE promoter. Conversely, cold competitors of ARE core plus GC (M1) and WT inhibited the binding of MafK to ARE, whereas those of ARE core alone (M5) inhibited the binding of MafK to ARE partially and cold competitors containing an AP-1-like element or GC box (M2, M3, M4, M6, M7) did not compete with this binding (unpublished). These data indicate that MafK bound both the ARE core and the GC box elements, but not the AP-1-like element, respectively.

Colocalization and recruitment of Nrf2, MafK, and JDP2 proteins to the ARE

To confirm the colocalization of Nrf2, MafK, and JDP2, we used Alexa Fluor 488 and Alexa Fluor 546 as secondary antibodies. Signals corresponding to Nrf2 were localized in the regions of decondensed chromatin and presented mainly as nuclear foci (unpublished). In contrast, the signals of JDP2 and MafK were detected in all regions of nuclei (unpublished). Most signals of Nrf2 and MafK colocalized with those of JDP2. Thus, a triple complex encompassing Nrf2, MafK, and JDP2 seems to be present in the nuclei of HeLa cells. This colocalization was confirmed using a chromatin immunoprecipitation (ChIP) assay, as described below.

ChIP experiments were performed to examine whether Nrf2, MafK, and JDP2 are recruited *in vivo* to the ARE of the HO-1 and NQO1 genes in WT or *Jdp2* KO MEFs. We designed specific primers capable of amplifying the AREs at either E1 or E2 sites, each of which contains multiple stress-responsive elements (BBRC 221, 570-576, 1996; 236, 313-322, 1997) and also contains a Maf-recognition element (MARE; Mol Cell Biol 14, 700-712, 1994). As shown in Figure 6C, without TPA induction, Jdp2 and MafK were recruited to the E1 and E2 sites in WT MEFs, but only MafK was recruited to the E1 and E2 sites in *Jdp2* KO MEFs. In response to TPA treatment (at 24 h), the recruitment of Nrf2, Jdp2, and MafK was significant in WT MEFs; however, only Nrf2 and MafK were recruited in *Jdp2* KO MEFs. Thus, the E1 and E2 sites may be critical for the differential regulation of Nrf2, MafK, and Jdp2 on the HO-1 enhancer, and JDP2 seems to be the key regulator of Mrf2/MafK recruitment and ARE response. Similar results were observed for the ARE of the NQO1 gene (**Figure 5**). Jdp2 was recruited to E1 of the NQO1 gene together with Nrf2 and MafK proteins in response to TPA in WT MEFs.

DISCUSSION

In this report, we showed that JDP2 upregulated the Nrf2/ARE signaling pathway with the cooperation of MafK under both basal and induced conditions via direct interaction with Nrf2. Based on the molecular data which were obtained, a regulatory interaction model that explains the manner via which JDP2 is able to upregulate the Nrf2-dependent antioxidant response, was also presented.

Moreover, JDP2 was critical for the generation of ROS and DNA oxidation and induced a cellular response to oxidative stress. Increased activation of the ROS metabolism was detected in *Jdp2* KO MEFs. In the case of *Jdp2* KO MEFs, the ROS metabolism and total levels of glutathione were increased, but the ratio of GSH/GSSG was decreased compared with that observed for WT MEFs, resulting in the promotion of a more oxidized environment. The level of ROS and 8-oxo-dGuo was also elevated in *Jdp2* KO MEFs compared with WT MEFs. Thus, these results indicate that JDP2 protects against intracellular oxidation, ROS activation, and DNA oxidation. Therefore, the response of the ARE-reporter gene and the DNA-binding activity of ARE were examined.

Analysis of Nrf2-null mutant mice showed that Nrf2 is a central regulator of the induction of many antioxidant-responsive genes and genes encoding phase II detoxification enzymes, and that Nrf2 is a key transcriptional activator of the ARE (BioEssays 2, 169-181, 2006). The Nrf2/ARE pathway is indispensable for the cellular defense system against oxidants, carcinogens, and inflammatory insults (Mol Cell Biol 26, 2773-3784, 2006; Cancer Res 66, 11580-11584, 2006; J. Exp Med 202, 47-59, 2005). Under normal physiological conditions, Nrf2 is captured in the cytoplasm by Keap1 and is turned over rapidly via proteasome degradation (Rapid Comm Mass Spec 22, 432-440, 2008; Cancer Res 60, 1426-1433, 2000; J Biol Chen 278, 2396-2402, 2003). However, in response to oxidative stress, Nrf2 is stabilized, relocates to the nucleus, forms heterodimers with a small Maf protein (either MafK, MafG, or MafF), and binds to and activates target antioxidant-response genes and genes encoding detoxification enzymes (Gene Dev 13, 76-86, 1999; Gene Cell 8, 379-391, 2003)

However, many reports have shown that addition of a small Maf protein to the transfection reaction leads to the repression of ARE reporter genes (J Biol Chem, 275, 15466-15473, 2000; 274, 26071-26078, 1999; 275, 40134-40141, 2000; 274, 33627-33636, 1999). No clear explanation was offered to clarify this discrepancy. Here, we identified the JDP2 transcription factor as a cofactor that enhanced the ARE activity, and observed that JDP2 bound to ARE and regulated the ARE-mediated transcription associated with the Nrf2/MafK factors. Analysis of the deletion of the JDP2 gene and the promoter assay of ARE showed that the bZIP domain of JDP2 was recruited to bind ARE core *in vitro*. The core sequence of the AREs from the NQO1 and HO-1 genes is TGACTCA, which matches fully the sequence of the JDP2-binding element (Mol Cell Boil 17, 3094-3102, 1997). These data suggest that JDP2 is a potential transcription factor in the regulation of ARE-mediated transcription. Here, we focused on the mechanism underlying the association of JDP2 with Nrf2/MafK to regulate ARE-dependent gene expression. We prepared a series of JDP2, Nrf2, and MafK deletion mutants to identify the domains involved in the binding of these factors to each other through basic zipper regions. The ChIP assay showed that the MafK/JDP2 complex was detected in WT MEFs in the absence of Nrf2. In addition, stimulation with TPA recruited Nrf2 to the MafK/JDP2 complex, which bound to the E1 and E2 sites of the HO-1 gene. Similarly, Nrf2 was not

recruited to the E1 site of the NQO1 gene in the absence of TPA; however, recruitment of Nrf2 was detected in the presence of TPA (**Figure 6**). Although Nrf2 was not a DNA-binding protein, the strong DNA-binding activity of this complex was evident after the association of Nrf2 with MafK or JDP2 or MafK/JDP2.

In response to oxidative stress, the complex of MafK might recruit Nrf2; however, but this complex did not stimulate ARE in *Jdp2* KO MEFs. In contrast, in the presence of JDP2, the JDP2/MafK heterodimer-mediated recruitment of Nrf2 induced the strongest ARE activity in WT MEFs (**Figure 6**). Although we cannot rule out the possibility of the involvement of the JDP2 homodimer and of the MafK homodimer and other complexes in WT MEFs in the enhancement of ARE activity, it is evident that JDP2 seems to play a crucial role as a positive cofactor of Nrf2/MafK in this process. The results of the ChIP assay were more significant. In WT MEFs, MafK and JDP2 were initially recruited to the ARE in the absence of TPA; in response to TPA, we identified Nrf2 as a coactivator that was recruited to form the ARE complex (**Figure 6**), which might enhance ARE reporter activity. However, in *Jdp2* KO MEFs, only MafK was recruited to the ARE, and TPA altered the recruitment of Nrf2 to the ARE, possibly to form the possible Nrf2/MafK complex (**Figure 6**). However, ARE reporter activity was lower in *Jdp2* KO MEFs, even in response to TPA because of the absence of JDP2. Taken together, these results led us to that JDP2 is critical for the induction of ARE activity in the presence of TPA (**Figure 7**). Here, we show an indirect evidence of the presence of triple complex of Nrf2/MafK/JDP2 by immunofluorescence study. It is also conceivable that JDP2 might help to stimulate the ARE activity of MafK/Nrf2, to convert the repressor function of this duplex (J Biol Chem 280, 32485-32492, 2005; J Biol Chem 274, 26071-26078, 1999; 275, 40134-40141, 2000; 274, 33627-33636, 1999) to the active stimulatory function.

Recently the role of ROS networks in inducing and maintaining senescence-induced tumor suppression was reported (Free Radic Biol Med 52, 7-18, 2012). Thus, the balance of ARE and ROS activity induced by JDP2 is critical for induction of senescence and tumor suppression. The SNP mutation and down-expression of JDP2 were reported in the patients of intracranial aneurysms and metastasis of pancreatic cancer (Neuroscience 169, 339-343, 2010; Inter J Biol Markers 25, 136-140, 2010). In each case the regulation induced by JDP2/Nrf2/MafK on ARE activity and ROS production might be involved.

In summary, our study demonstrated that JDP2 binds ARE and enhances the ARE-dependent gene expression associated with the Nrf2/MafK factors. These findings suggest that JDP2 plays a potential role in protecting cells or tissues against the malicious attack of exogenous carcinogens and/or endogenous reactive oxygen/nitrogen species, by inducing several detoxifying/antioxidant enzymes. Therefore, JDP2 acts not only as an AP-1 repressor protein, to suppress cell proliferation during cancer progression, but also participates in maintenance of ROS homeostasis to prevent cell

damage by ROS.

---

1. Wang, S-W., Lee. J-K., Ku C-C., Chiou S-S., Lin S. C-L., Ho M-F., Wu D-C., and Yokoyama, K.: Jun dimerization 2 in oxygen restriction; control of senescence. **Curr. Pharmaceutical Design 17**, 2278-2289 (2011) [**Cover of the Journal**].

2. Saito, S., Wang, S-W., Ku, C-C., Lin, C-H., Wu, D-C., Maruyama. Y., and Yokoyama, K.; Human amnion-derived pluripotent stem cells as a promising source for regenerative medicine and tissue engineering. **J. Bioengineering & Biomedical Sciences** in press (2012).

3. Abei, M., Fukuda, K., Seo, E., Wakayama, M., Kawashima, R., Murata, T., Obata, Y., Hamada, H., Yokoyama, K., and Hyodo I. Various gene therapy strategies for biliary cancers using oncolytic, tropism-modified, armed, combination, and targeted adenoviruses. **Current Cancer Drug Targets** in press (2012).

4. Hsiao, H., Huang, S-E., Ku, C-C, and Yokoyama, K.: International Society for Stem Cell Research 2011, ninth annual meeting in Toronto (June 15-June 18, 2011). **Kaohsiung Journal of Medical Sciences 28**, 296-298 (2012).

5. Huang, S-E., Hsiao, H., Ku, C-C, and Yokoyama, K.: Cold Spring Harbor Asia/International Society for Stem Cell Research 2011 meeting; Cellular programs and reprogramming (October 24-28, 2011). **Kaohsiung Journal of Medical Sciences 28**, 352-354 (2012).

6. Chen, C-W., Chen, T-Y., Tsai L-L., Lin C-L., Yokoyama, K., Lee, W-S., Chiueh. C. C., and Hsu, C.: Inhibition of autophagy as a therapeutic strategy of iron-induced brain injury after hemorrhage. **Autophagy** in press.

7. Darlyuk-Saadon, I., Weidenfeld-Baranboim, K., Yokoyama, K., Hai T., and Aronheim, A.; The bZIP repressor proteins, the c-Jun dimerization protein 2, and the Activating Transcription factor 3, recruit multiple members of HDAC to the ATF3 promoter. **Biochim. Biophys. Acta** in press.

8. Saito, S., Lin, Y-C, Murayama, Y., Hashimoto, K., and Yokoyama, K.; Human amnion-derived cells as a reliable source of stem cells. **Current Medical Medicine** in press.

9. Yokoyama, K. and Kuo Kun-Kai.; Role of chromatin-remodeling factor JDP2 in cellular senescence. **Tumor Dormancy and Cellular Quiescence and Senescence**. Volume 2, ed. by Hayat, M. A. Springer Science, USA. In press.

10. Tanigawa, S., and Yokoyama, K.: JDP2 is a cofactor of antioxidant regulatory complex and participates in ROS homeostasis. **Introduction to genetic (DNA methylation and gene regulation)**. Book, ed. by J. Wan, iConcept press, USA. In press.

11. Tanigawa, S., Lee, C-H., Hasegawa, H., Kawahara, A., Korenori. Y., Qin, S., Niguchi, M., Miyamori, K., Lee, L-H., Lin Y-C., Lin, S. C-L., Chiou, S-S., Nakamura, Y., Jin C., Yamaguchi, N., Eckner, R., Hou, D-X., and Yokoyama, K.: Transcription factor JDP2 is a novel key component of the Nrf/MafK complex regulating the response to ROS homeostasis. Submitted.

---

2. The potential of our research

We are also interested in the acetylation of histones, cell proliferation, differentiation, senescence and cancer development. We have used embryonic carcinoma and embryonic stem cells to study the role of AP-1 family, such as ATF-2 and JDP2, in cell differentiation, cellular senescence and the cell cycle, which seems to be involved in crosstalk between the p53 and Rb pathways. We have selected a human medulloblastoma as a model system to understand how JDP2 involved in generating the tumor. We recently reported that JDP2 controls the transcription of cyclin A2, and its defects results in cell cycle arrest, which implies that JDP2 plays a role in oncogenesis. Therefore we propose to study the mechanism of how JDP2 regulates cell cycle arrest via its activity in transcriptional and post-transcriptional regulation. JDP2 is a novel sequence-specific transcription factor with histone binding activity that inhibits HAT and histone methylation and nucleosome assembly activity in a similar way to histone chaperones. Moreover, we will evaluate the possibility of using JDP2 as a therapeutic target in cancer and generate a mouse model of meduloblastoma using JDP2 KO mice. We believe that this proposal will unveil a novel mechanism for the transcriptional epigenetic regulation of cell cycle progression as well as have implications for cancer therapy.